Atmos. Meas. Tech. Discuss., 4, 2789–2826, 2011
www.atmos-meas-tech-discuss.net/4/2789/2011/
doi:10.5194/amtd-4-2789-2011

Atmospheric Measurement Techniques Discussions

First national intercomparison of solar ultraviolet radiometers in Italy

H. Diémoz[1,2], A. M. Siani[2], G. R. Casale[2], A. di Sarra[3], B. Serpillo[4], B. Petkov[5], S. Scaglione[3], A. Bonino[6], S. Facta[6], F. Fedele[7], D. Grifoni[8], L. Verdi[9], and G. Zipoli[8]

[1]ARPA Valle d'Aosta, Aosta, Italy
[2]Sapienza – University of Rome, Department of Physics, Roma, Italy
[3]ENEA, UTMEA-TER, Roma, Italy
[4]ARPA Basilicata, Potenza, Italy
[5]CNR-ISAC, Bologna, Italy
[6]ARPA Piemonte, Ivrea, Italy
[7]ARPA Puglia, Bari, Italy
[8]CNR-IBIMET/LaMMa, Firenze, Italy
[9]APPA Bolzano, Bolzano, Italy

Received: 14 March 2011 – Accepted: 9 May 2011 – Published: 11 May 2011

Correspondence to: H. Diémoz (h.diemoz@arpa.vda.it)

Published by Copernicus Publications on behalf of the European Geosciences Union.

Abstract

A blind intercomparison of ground-based ultraviolet (UV) instruments has been organized for the first time in Italy. The campaign was coordinated by the Environmental Protection Agency of Aosta Valley (ARPA Valle d'Aosta) and took place in Saint-Christophe (45.8° N, 7.4° E, 570 m a.s.l.), in the Alpine region, from 8 to 23 June 2010. It involved 8 institutions, 10 broadband radiometers, 2 filter radiometers and 2 spectroradiometers. Synchronized measurements of downward global solar UV irradiance at the ground were collected and the raw series were then individually processed by the respective operators on the basis of their own procedures and calibration data. The comparison was performed in terms of global solar UV Index and integrated UV-A irradiance against a well-calibrated double monochromator spectroradiometer as reference. An improved algorithm for comparing broadband data and spectra has been developed. For some instruments, we found average deviations ranging from −16 % up to 20 % relative to the reference and diurnal variations as large as 15 % even in clear days. Remarkable deviations also arose from instruments recently in operation and never involved in field intercomparison.

1 Introduction

The last two decades have witnessed a worldwide diffusion of ground-based instruments for measuring the solar ultraviolet (UV) radiation reaching the Earth surface. Many radiometers have been employed to investigate the influence of atmospheric composition changes on solar UV irradiance at the ground (WMO, 2011) as well as to assess the related risks for the human health and the environment (Lucas et al., 2010; UNEP, 2010).

However, high quality UV measurements are still a complex task. Possible UV trends are expected to be small and may be masked by natural cycles (Seckmeyer et al., 2001; McKenzie et al., 2003; Glandorf et al., 2005; Seckmeyer et al., 2009). Moreover,

AMTD

4, 2789–2826, 2011

measurements carried out within monitoring networks, in particular when made with different instruments, should reveal actual environmental patterns and should not be biased by instrumental differences. Thus, a great effort must be dedicated to achieve the necessary accuracy, both in developing and in maintaining the instruments. Therefore, data processing, calibration procedures, quality assurance and quality control (QA/QC) methods are of primary importance (Bernhard and Seckmeyer, 1999; Bernhard et al., 1998; di Sarra et al., 2002).

Special care has been dedicated to define useful guidelines for quality control of UV monitoring (Webb et al., 1998, 2003; Seckmeyer et al., 2008a; Webb et al., 2006). Travelling instruments have been developed (Gröbner et al., 2005) and several calibration facilities exist nowadays (Gröbner et al., 2002, 2006). Moreover, some instrument comparisons have been organized all over the world (Leszczynski et al., 1998; Bais et al., 2000, 2001; Gröbner et al., 2007; Lantz et al., 2002, 2008) and have proven to be very successful in pointing out instrumental malfunctioning or data processing inaccuracies.

Continuous monitoring of solar UV radiation in Italy began in the early 1990s (Casale et al., 2000; Ialongo et al., 2008). The relatively wide latitude range over which Italy extends and its large variety of environments, which is representative of the Mediterranean as well as the Alpine regions (Meloni et al., 2000), make solar measurements in this country very valuable. Furthermore, sun exposure among natives and tourists is very common in both work and leisure activities (Siani et al., 2008, 2009). Some Italian institutions have been involved in European projects (Seckmeyer et al., 2008b), COST Actions (Hülsen and Gröbner, 2007) and international campaigns (Gröbner et al., 2010) and several Regional Environmental Protection Agencies (ARPAs) started a monitoring programme in the last few years. However, the existing Italian instrumentation is not being operated within an established national network and a common research programme has not yet been planned. Only few and limited comparisons have been already performed (Di Menno et al., 2002), while a comprehensive national intercomparison had never been organized so far. Hence, the results of this first campaign are fundamental to assess the overall accuracy of the Italian instrumentation and to take measures to improve it if needed. Moreover, the campaign gives also additional information about the effectiveness of different correction procedures and the accuracy of calibration coefficients.

The paper is organized as follows: the participating instruments and the radiative transfer model are described in Sect. 2. Section 3 gives an overview of the campaign. Section 4 presents the methods used to compare measurements from different instruments. The results are shown and discussed in Sect. 5. Finally, conclusions are drawn in Sect. 6.

2 Participating instruments

All the instruments participating to the campaign provided measurements of global solar UV irradiance. A description of the Bentham reference spectroradiometer, the Brewer spectrophotometer, broadband and narrowband radiometers is given in the following along with information about calibration and processing procedures. Table 1 summarizes the participating instruments and agencies, the identification numbers (id) used in the campaign, the calibration references to which the instruments are traceable and the corrections applied to the data.

2.1 Bentham double monochromator spectroradiometer

A commercially available Bentham DTMc300F spectroradiometer belonging to ARPA Valle d'Aosta was used as the reference of the comparison (id 00). Similar instruments were described in detail elsewhere (Gröbner et al., 2005). The original optics were replaced with a PTFE special shaped diffuser (CMS-Schreder, Model UV-J1002), which is temperature-stabilized and characterized by a nearly perfect angular response (Schreder et al., 1998; Gröbner and Blumthaler, 2007), so that no angular correction is needed. A spectral scan from 290 to 400 nm every 0.25 nm takes about 3 min and was repeated every 5 min throughout the campaign.

AMTD
4, 2789–2826, 2011

The spectroradiometer calibration is regularly performed by ARPA Valle d'Aosta using a triad of 200 W QHT lamps calibrated at the Physikalisch-Meteorologisches Observatorium Davos – World Radiation Center (PMOD-WRC) with reference to the QASUME scale traceable to PTB (Gröbner and Sperfeld, 2005). The lamps and the diffuser are fitted in a portable field calibrator. An active feedback loop kit consisting in a calibrated shunt, a programmable power supply (Xantrex XPD 33-16) and a digital multimeter (Agilent 34970A) controls the 6.300 A current feeding the calibrator with an uncertainty lower than 1 mA. The spectroradiometer was compared to QASUME in 2009 showing an average offset of 0 % and diurnal variations below 2 % on clear sky days (http://www.pmodwrc.ch/euvc/euvc.php?topic=qasume_audit). Table 2 summarizes the combined radiometric uncertainty calculated for different wavelengths according to Gröbner et al. (2005); Bernhard and Seckmeyer (1999) and the Guide to the expression of Uncertainty in Measurement (JCGM, 2008).

The spectroradiometer was calibrated at the beginning and at the end of the comparison. In addition, two intermediate calibrations were performed weekly during the campaign. Figure 1 presents the variations of the spectral responsivity, which are below the radiometric uncertainty of 3 %. In order to reduce the errors caused by a wavelength misalignment, the spectra were processed with the SHICrivm package (Williams et al., 2003) using the instrumental slit function (measured with a He-Cd laser in 2009).

The total combined uncertainty is reported in Table 3 for different wavelengths and solar zenith angles.

2.2 Brewer spectrophotometer

A detailed description of the Brewer spectrophotometer and its principles of operation is provided by Kerr et al. (1980); Kerr (2010). The Brewer MKIV #066 (id 11) has been measuring total column ozone (which is necessary for the spectral corrections of several broadband radiometers and as an input parameter to the model) for the campaign period. It was also included in the comparison as a tested instrument to measure solar UV irrandiance.

Global irradiance spectra from 290 to 325 nm in steps of 0.5 nm were recorded every 30 min. Even though it was possible to synchronize Brewer and Bentham spectral measurements wavelength by wavelength (as usually done during the regular Brewer calibrations against the Bentham, see below), we decided to give priority to collect a large number of Bentham measurements and to compare the data recorded by the two instruments as described in Sect. 4. The Brewer slit function is nearly triangular with a FWHM of about 0.63 nm (measured with a He-Cd laser in 2009). An algorithm similar to the one developed by Cheymol and De Backer (2003), together with data from an in-situ Langley Plot calibration, is regularly employed to retrieve the aerosol optical depth (AOD) at 320 nm from clear-sky UV direct irradiance. The AOD is later included in the radiative transfer calculations.

The global irradiance scale of the Brewer is calibrated monthly against the ARPA Valle d'Aosta Bentham spectroradiometer by recording synchronous spectra during several clear days. Every two years, the Brewer is compared to the QASUME travelling standard. The spectra from the Brewer are corrected for its angular response, temperature, straylight and wavelength shifts. The ozone scale is calibrated with reference to the travelling standard #017 from International Ozone Services every two years.

2.3 Broadband radiometers

Ten broadband filter radiometers (id 01-10) participated to the comparison campaign. The output voltage of instruments 01-08, roughly proportional to the weighted irradiance to be measured (details are provided in the next paragraph), has been recorded with a digital programmable multimeter. A sampling time of 10 s was chosen for analog measurements. Data were collected also at night-time for finding electrical instabilities and calculating a zero-offset for each instrument. Two radiometers (id 09-10) were digital models equipped with their own acquisition systems, which recorded the (averaged) data at a maximum frequency of one value every 5 min. Four double-band radiometers measured simultaneously UV-A and erythemally weighted irradiance in

AMTD
4, 2789–2826, 2011

First intercomparison of UV radiometers in Italy

H. Diémoz et al.

two distinct channels. The remaining were single-band models (erythemal weighting). All broadband instruments were temperature-stabilized.

2.3.1 Calibration and processing of broadband radiometers

Ideally, the output voltage of the broadband radiometers should be perfectly proportional to the convolution of the solar spectral irradiance with a weighting curve, namely the sensitivity of the human skin (erythemal action spectrum, CIE, 1998; Webb et al., 2011) or a UV-A (315–400 nm) unitary function (CIE, 1999). In that case, an absolute calibration factor could be assessed to convert the voltage to the irradiance. However, the instrumental spectral sensitivity always differs from the action spectrum. Moreover, the angular response does not perfectly coincide with a cosine function. The induced errors may be relatively high and many methods can be applied to the recorded data to overcome the problem. Some of them are described in the following.

Data obtained by some instruments (id 01-06) were reprocessed by their respective agencies with a multiplicative factor stored in a table (matrix) and depending on the total ozone, as measured by the Brewer throughout the campaign, and the solar zenith angle at the time of measurement (Webb et al., 2006; Gröbner et al., 2007). In such a way, spectral and angular corrections could be easily introduced. More precisely, data from radiometers 01-03 were processed with a matrix calculated by the owner agency with reference to the ARPA Valle d'Aosta Bentham spectroradiometer and using a spectral and angular characterization performed by the PMOD-WRC. Data from radiometers 04 and 05 were processed with a matrix provided by the manufacturer. Data from the radiometer 06 were processed with a matrix calculated by the PMOD-WRC during the COST Action 726, in 2006. A fixed correction factor was used with instruments 07 and 09-10. The former was calibrated with reference to the QASUME travelling standard during a spectroradiometer comparison in 2008. Radiometers 09-10 were calibrated by the manufacturer in 2010. Finally, instrument 08 used the algorithm developed by Bodhaine et al. (1998) and was calibrated with reference to Brewer #123 (which is in turn traceable to NIST) belonging to the Italian national agency for new technologies, energy and sustainable economic development (ENEA).

2.4 Narrowband radiometers

The narrow-band filter radiometer UV-RAD (id 12) has been designed and developed at the Institute of Atmospheric Sciences and Climate (ISAC) of the Italian National Research Council (CNR), as part of a cooperative program with ENEA. The UV-RAD is able to measure the solar UV irradiance in seven channels centered at 300, 306, 310, 314, 325, 338 and 364 nm wavelengths with FWHM varying from 0.7 to 1 nm. The overall scan of the channels takes about 90 s. Further details about the instrument are given by Petkov et al. (2006). The UV-RAD radiometer was calibrated by comparison against two Bentham spectroradiometers traceable to international standards: a first campaign was organized in Alomar (Norway) in 2004; a second comparison was performed in Saint-Christophe (Italy) in 2006. The measurements recorded by UV-RAD allow the retrieval of column ozone applying the method developed by Stamnes et al. (1991). To reconstruct the UV spectral irradiance at the ground, the atmospheric transmittance was assessed at the measured wavelengths and the spectrum was evaluated through a radiative transfer model at the time of observation, using the retrieved total ozone as an input.

The F-RAD radiometer (id 13) has been developed by ENEA. It operates on 13 wavelengths from about 281 to 378 nm which are selected by as many filters characterized by a FWHM from 0.5 to 1.3 nm. Each filter is manufactured by the Optical Components Group of Enea using ion-assisted vapour-phase evaporation. This technique ensures an excellent stability in time. The radiometer is equipped with a GPS receiver for time synchronization and is temperature-stabilized to ±0.5° C using a Peltier cell. The overall scan of the channels takes about 1 min. The calibration of F-RAD was performed in two steps. At first, a field calibration system developed by NIST and NOAA (Early et al., 1998) which uses several 1000 W FEL lamps traceable to NIST was used. Then, the F-RAD measurements were compared with simultaneous co-located spectra from

Brewer #123 obtained during three months at the ENEA observatory in the Lampedusa island (Southern Italy). Brewer #123 is regularly calibrated with the field calibrator and was characterized for its cosine response (Bais et al., 2005) and slit function. The spectra used in the comparison were reconstructed from narrowband irradiances using the Tropospheric Ultraviolet and Visible (TUV) radiation model (Madronich, 1993).

2.5 Radiative transfer calculations

A radiative transfer model, the libRadtran package (Mayer and Kylling, 2005), was used in the campaign for comparing different kind of data as explained in Sect. 4 and as a further quality control. Table 4 summarizes the data set entered as input to the model. The diffuse irradiance was scaled by 95 % accounting for the mountain horizon, as explained by Diémoz and Mayer (2007). The simulated spectra were then treated similarly to the instrumental data (id 14 was assigned to the model) and compared to the reference.

3 Campaign overview

3.1 Campaign protocol

Every participating agency was asked to send a calibrated radiometer to the organizers or, in case of complex instrumentation, to assist with a specialized operator. The campaign began on June 8 (day of year 159) and ended on June 24 (day of year 175), comprising days across the summer solstice, thus allowing measurements at a large range of solar elevations. Synchronous measurements of solar irradiance were collected for the whole time period. Every instrument (or computer connected to an instrument) was synchronized to the same reference through the Internet Network Time Protocol or a GPS signal. The quartz domes of the radiometers were cleaned and the horizontal leveling was checked every morning before sunrise.

AMTD
4, 2789–2826, 2011

At the end of the campaign, the raw series (e.g. the series of the recorded voltages, for the broadband radiometers) were individually reprocessed by the respective operators using the same algorithm and calibration data usually employed by each agency. The data were then sent to ARPA Valle d'Aosta for the comparison in terms of the global solar UV Index (Vanicek et al., 1999) or broadband UV-A irradiance.

3.2 Site description

The site of Saint-Christophe (45.8° N, 7.4° E, 570 m a.s.l.) is located in Northwestern Italy, in the Alpine region. It was chosen because of the presence of state-of-the-art instruments necessary for the comparison: a spectroradiometer traceable to international standards and a calibrated Brewer spectrophotometer. The site is also characterized by low pollution levels. Even though Saint-Christophe lies in a valley bottom, the horizon is free enough to allow meaningful solar measurements. Figure 2 shows the horizon at the intercomparison site, together with the daily course of the sun position for 8 June 2010. Anyway, data recorded when the sun was behind the mountains were removed from the analysis. The sunrise was at about 5 UT and the sunset at about 18 UT during the campaign. The minimum solar zenith angle was 22.3° corresponding to the summer solstice.

3.3 Atmospheric conditions

Cloudy sky accompanied the first part of the campaign. Some showers occurred in the period from June 9 to 17. Data recorded under rainy conditions were removed from the analysis. The last four days (21–24 June) were almost clear and the maximum UV Index was about 8, which is a typical value for the site of Saint-Christophe in summer.

AMTD
4, 2789–2826, 2011

4 Methods

The methods used to compare the UV data recorded by the various instruments against the reference are described below.

4.1 Analog broadband radiometers

The weighted and integrated irradiance measured with a broadband radiometer can be expressed in the following general form, provided that appropriate angular and spectral corrections are applied to the data:

$$I_{\mathrm{CIE}}(t) = \int_{280}^{400} I(\lambda,t)\mathrm{CIE}(\lambda)d\lambda \quad (1)$$

CIE(λ) being a standardized action spectrum (the erythemal spectrum (CIE, 1998) or the UV-A unitary function between 315 and 400 nm; CIE, 1999) and $I(\lambda,t)$ the solar spectral irradiance at the ground at time t. Unfortunately, as already stated in the previous sections, we are not able to measure the instantaneous value of $I(\lambda,t)$, since a full scan of the spectroradiometer takes about 3 min. Hence, following previous studies (Gröbner et al., 2007; Hülsen and Gröbner, 2007), it was decided to downscale the temporal resolution of the broadband data to optimize the comparison with the spectral measurements and an appropriate algorithm was developed.

The procedure followed during COST Action 726 was based upon the determination of the detector-weigthed broadband irradiance I_{SRF} from spectroradiometric measurements:

$$I_{\mathrm{SRF}} = \int I_{\mathrm{SP}}(\lambda,t(\lambda))\mathrm{SRF}(\lambda)d\lambda \quad (2)$$

where SRF(λ) is the spectral response function of the detector and I_{SP} is the spectral irradiance at wavelength λ actually recorded by the spectroradiometer at time $t(\lambda)$. It

AMTD
4, 2789–2826, 2011

should be noticed that wavelength and time are no longer independent variables. Then, the most representative timestamp t_{SRF} was calculated using a weighted average as

$$t_{\mathrm{SRF}} = \frac{\int t(\lambda) I_{\mathrm{SP}}(\lambda, t(\lambda)) \mathrm{SRF}(\lambda) d\lambda}{\int I_{\mathrm{SP}}(\lambda, t(\lambda)) \mathrm{SRF}(\lambda) d\lambda} \tag{3}$$

where $t(\lambda)$ is the time at which the spectroradiometer measures the irradiance at wavelength λ. In the COST campaign, a downscaled broadband signal was obtained from individual voltage measurements $u(t)$ as

$$u_{\mathrm{SRF}} = \frac{\int u(t(\lambda)) I_{\mathrm{SP}}(\lambda, t(\lambda)) \mathrm{SRF}(\lambda) d\lambda}{\int I_{\mathrm{SP}}(\lambda, t(\lambda)) \mathrm{SRF}(\lambda) d\lambda} \tag{4}$$

The calibration factor was derived successively using u_{SRF} and the angular correction function.

However, since the actually measured spectral irradiance $I_{\mathrm{SP}}(\lambda, t(\lambda))$ is used in the weighted average in Eqs. (3) and (4), the downscaled signal u_{SRF} is more influenced by values of $u(t)$ registered in clear sky conditions (larger I_{SP} values) and less sensitive to measurements in presence of clouds (lower I_{SP} values). As a consequence, the algorithm tends to slightly overestimate the downscaled irradiance in cloudy conditions.

In order to avoid this effect, we substituted the measured irradiances I_{SP} with modeled clear sky irradiances $I^0_{\mathrm{SP}}(\lambda, t(\lambda))$. In addition, we used calibrated and cosine-corrected broadband irradiances instead of measured signals from the broadband radiometers. Equation (4) was rewritten as

$$I_{ds} = \frac{\int I_{\mathrm{BB}}(t(\lambda)) I^0_{\mathrm{SP}}(\lambda, t(\lambda)) \mathrm{CIE}(\lambda) d\lambda}{\int I^0_{\mathrm{SP}}(\lambda, t(\lambda)) \mathrm{CIE}(\lambda) d\lambda} \tag{5}$$

where I_{ds} is the downscaled broadband irradiance, $I_{\mathrm{BB}}(t(\lambda))$ are the CIE-weighted broadband irradiances reprocessed by the operators and $I^0_{\mathrm{SP}}(\lambda, t(\lambda))$ is the modeled clear sky irradiance at the time at which the reference instrument is measuring the wavelength λ.

AMTD
4, 2789–2826, 2011

Assuming that clouds approximately act as a *grey filter*:

$$\frac{I_{\mathrm{BB}}(t)}{I^0_{\mathrm{BB}}(t)} \approx \frac{I_{\mathrm{SP}}(\lambda,t)}{I^0_{\mathrm{SP}}(\lambda,t)} \quad \forall\lambda \tag{6}$$

and that the integrated clear sky irradiance I^0_{BB} does not change appreciably during a spectral scan, we obtain

$$I_{ds} \approx \int I_{\mathrm{SP}}(\lambda,t(\lambda))\mathrm{CIE}(\lambda)d\lambda \tag{7}$$

The right-hand term is the CIE-weighted irradiance value as measured by the reference instrument in a scan time.

Thus, the comparison for broadband radiometers consisted in analyzing the series of ratios between the downscaled broadband irradiances in Eq. (5) and the convoluted reference spectra in Eq. (7). The implementation of the algorithm used look-up tables (previously calculated with libRadtran) to quickly obtain the appropriate modeled irradiance.

The timestamp relative to the downscaled irradiance was calculated as

$$t_{ds} = \frac{\int t(\lambda)\mathrm{CIE}(\lambda)I^0_{\mathrm{SP}}(\lambda,t(\lambda))d\lambda}{\int \mathrm{CIE}(\lambda)I^0_{\mathrm{SP}}(\lambda,t(\lambda))d\lambda} \tag{8}$$

The results of the improved algorithm are presented in Sect. 5.

4.2 Digital broadband radiometers, narrowband and spectral instruments

The previous algorithm was not applicable to digital broadband radiometers (id 09-10), narrowband (id 12-13) and spectral instruments (id 11), since measurements were taken at a too low frequency. Instead, a simple interpolation was used to compare data at the right time. The spectra obtained by the reference, the Brewer and the narrowband radiometers were weighted and integrated and a timestamp was assigned to

AMTD
4, 2789–2826, 2011

the obtained values following Eq. (8). Timestamp of the digital radiometers was set to the middle of the sampling time. The user and the reference series were then appropriately interpolated (the series sampled at the highest frequency was interpolated to the other) and the ratios between the series were calculated. Care was taken to avoid interpolation in case of too large time intervals (1 min for narrowband radiometers and 5 min for the Brewer).

The spectral irradiances obtained with narrowband radiometers and the Brewer were also analysed in detail to assess the behaviour of the instruments at different wavelengths. However, spectral ratios are not presented here, since beyond the scope of this paper.

5 Results and discussion

Figure 3 shows the time series of the measurements recorded by the Bentham spectroradiometer, in terms of global solar UV Index and broadband UV-A irradiance. Cloudy days are clearly visible in the first part of the campaign (days of year 159 to 171).

The ratios between the measurements made by each instrument and the reference were then analyzed. Figure 4 presents a comparison of several methods to downscale the data from broadband radiometers during three cloudy days. First, the ratios derived interpolating the broadband values to the most representative time of the reference spectra using a cubic spline are shown. As can be seen from the figure, the results obtained in cloudy conditions are not optimal and present some fictitious fluctuations. The new algorithm developed in this study is less influenced by clouds than both the spline interpolation and the COST Action 726 algorithm.

We decided to use the median and the interquartile range (IQR) to describe the statistical distributions of the ratios, which are not normally distributed and show many outliers. The former is a measure of the central tendency of a sample and the latter is a measure of dispersion. Boxplots (Figs. 5 and 6) summarize the results during clear sky days (days 172 to 175).

AMTD
4, 2789–2826, 2011

5.1 Relative deviations from the reference under clear sky conditions

We first analyze the median values of the ratios between the radiometers and the reference (Figs. 5 and 6). Remarkable differences may be noticed among the instruments: the differences relative to the reference spectroradiometer range from −16 % (instruments 12 and 13) up to 19 % (instrument 4) for the UV Index series. It is interesting to observe that UV-A data from double-band radiometers show similar patterns, denoting an internal consistency in all instruments. It has to be noticed that even radiometers recently calibrated by the respective manufacturers present significant deviations (instruments 04, 05, 09, 10). Some radiometers, along with the reference, share the same calibration standard (PMOD/QASUME) and this is clearly depicted in the graphs: instruments 01, 02, 03, 06, 07, 11 show median ratios of about 1. In particular, it must be emphasized that radiometers 01, 02 and 03 and the Brewer (id 11) were all calibrated against the Bentham and this exercise provides information on the radiometers stability and reliability of the angular corrections.

The values obtained with radiometer 08 are consistent with the results of previous comparison between the ENEA instrumentation and QASUME (the former overestimates QASUME by about 5 %) (Gröbner et al., 2006). The large discrepancies of the UV-RAD (id 12) may be ascribed to deterioration of the internal components (e.g. filters, O-ring) and drift in calibration. Narrowband radiometer 13 was thoroughly examined after the campaign and a sealing defect was discovered which let humidity and dust enter the instrument (thus decreasing its sensitivity). Finally, although the radiative model (id 14) was configured with few basic parameters, the results are rather satisfying: the difference relative to the reference is −0.3 % for the UV Index and −1.2 % for the broadband UV-A irradiance.

5.2 Daily variability in clear sky conditions

Every instrument shows a different IQR in clear sky days as presented in Figs. 5 and 6. Most of the total variability for clear sky conditions, as we will see later, is to ascribe to daily (not day-to-day) variability, since the ratios distinctly depend on the solar elevation. To investigate the angular dependence, the ratios were plotted against the solar zenith angle (Figs. 7 and 8) for the morning and the afternoon separately for clear sky days.

The ratios from the series processed with state-of-the-art algorithms (i.e. matrix of coefficients) are characterized by lower daily variability (id 01 to 06). On the contrary, radiometer 07, whose median was close to unity, shows very clear angular dependence and the largest IQR for clear sky (10 %). Indeed, since a single constant factor has been used for the conversion from the electric signal to the irradiance, angular and spectral errors are not considered. This is also the case of radiometers 09 and 10, which, however, exhibit a better cosine response than 07. Similarly, the ratios for radiometer 08 show a particular shape. The corrections applied to that radiometer use an empirical function obtained by comparison with Brewer #123. It must be emphasized that the ratio is reasonably constant at solar zenith angles lower than 70° and most of the deviations appearing in Fig. 5 are due to measurements at larger solar zenith angles. An incorrect determination of Brewer #123 cosine response at large incidence angles or of the spectral sensitivity of the broadband radiometer could be responsible for the strange behaviour. Further investigations are being carried out. The daily variability of the Brewer spectrophotometer (id 11) is within the limits of the uncertainty of the radiative model used for the correction and the instrumental uncertainty. The angular dependence of the narrowband radiometer 13 is pronounced only for zenith angles above 60°. This behaviour should be probably investigated in detail.

The daily variability of the model is comparable to the uncertainty of other instruments. This shows that both model and reference instrument are consistent.

5.3 Morning/afternoon asymmetry

Several instruments present an asymmetry between the morning and the afternoon ratios. For some of them (id 01, 04, 06, 12) the difference between the morning and afternoon ratios is very small (less than about 2 %) and may be ascribable to the deterioration or misalignment of the leveling bubble (id 01), to a slight azimuthal dependence (already noticed e.g. for radiometer 06 during the COST Action 726 campaign) as well as to the effect of the internal temperature or humidity.

The morning/afternoon change is slightly higher for radiometer 05, about 3 %. The difference is clearly visible also in the unprocessed series of voltages, so that an error relating to the processing can be easily excluded. An asymmetry of about 4 % is also present in the Brewer ratios. However, the variation is not explainable neither by an azimuthal dependency (the Brewer turns on its axis during the day and follows the solar azimuth) nor by a leveling problem (the spectral ratios, not presented here, reveal that the Brewer asymmetry is higher for the lowest wavelengths). Unaccounted temperature and humidity effects may be responsible for this behaviour.

5.4 Effect of clouds

The effect of clouds on the ratios can be examined taking into account the series of measurements recorded in the whole campaign period (days 159 to 175), in both cloudy and clear days (Figs. 9 and 10). While median values do not change appreciably, the full range of the ratios increases noticeably and in many cases exceeds ±10 %. This is to ascribe to many factors. First, the cosine corrections were calculated on the hypothesis of clear sky. Thus, for similarly processed series, the radiometers with a good cosine response (i.e. with a smooth matrix), for example id 01, 02, 04 and 05, show slightly better performances compared to the others, e.g. id 03 and 06. Second, time interpolations between measurements produce large deviations. This is the case of instruments 09 to 11 and, to a lesser degree, 12 and 13.

Finally, it is interesting to notice that the error is amplified by the processing algorithms used with radiometers 07 and 08. In those cases, the full range of the ratios may exceed ±20 % or even ±30 %.

6 Summary and conclusions

This study was stimulated by the need to assess the accuracy of the Italian UV measurements in order to plan a future national network which will be able to guarantee reliable and homogenized data. 14 instruments belonging to 8 different agencies participated to the campaign. The comparison lasted in total 17 days characterized by cloudy and clear skies. About 3000 irradiance spectra and 140000 samples were collected respectively for each spectral/narrowband and broadband instrument. The data obtained by the tested instruments were compared to a well-calibrated Bentham double monochromator spectroradiometer. The results were presented in terms of ratios between the user instruments and the reference. An optimized algorithm was specially developed to compare high-frequency broadband measurements with reference spectra. Average deviations ranging from −16 % to +19 % and interquartile ranges up to 10 % even for clear sky days were discovered and discussed. These values are very large compared to the uncertainty of state-of-the-art instruments. Moreover, they are greater than the expectations of the respective operators. However, out of the 13 instruments which were compared to the reference spectroradiometer, eight show median and interquartile ratios which are within ±10 % of the reference; five are within ±5 %. The ratios from the libRadtran radiative model, which was configured with few basic parameters, are satisfying and within few percents of the reference under clear sky conditions. The intercomparison also allowed the identification of a sealing defect of one of the narrowband radiometers and possible problems in the cosine correction of some instruments.

Consistent efforts to improve the calibration of the instruments and the processing algorithms are essential and should be made before deciding to set up a national network. The results highlight the importance of intercomparisons, which could be repeated every few years, also to assess the effects of the forthcoming corrective actions.

All data from the intercomparison are freely downloadable from www.uv-index.it for further research purposes.

AMTD
4, 2789–2826, 2011

Acknowledgements. The authors would like to thank S. Saudino and S. Martorina from ARPA Piemonte, F. Sabatini from IBIMET-CNR/LaMMa, I. Di Sarcina and F. Menchini from ENEA, V. Lanorte from ARPAB for their valuable help with the campaign, the calibration and data processing of the instruments.

References

Bais, A., Topaloglou, C., Kazadtzis, S., Blumthaler, M., Schreder, J., Schmalwieser, A., Henriques, D., and Janouch, M.: Report of the LAP/COST/WMO Intercomparison of Erythemal Radiometers, Thessaloniki, Greece, Tech. rep., World Meteorological Organization – Global Atmospherere Watch, 1–54, 2000. 2792

Bais, A. F., Gardiner, B. G., Slaper, H., Blumthaler, M., Bernhard, G., McKenzie, R., Webb, A. R., Seckmeyer, G., Kjeldstad, B., Koskela, T., Kirsch, P. J., Gröbner, J., Kerr, J. B., Kazadzis, S., Leszcznski, K., Wardle, D., Josefsson, W., Brogniez, C., Gillotay, D., Reinen, H., Weihs, P., Svenoe, T., Eriksen, P., Kuik, F., and Redondas, A.: SUSPEN intercomparison of ultraviolet spectroradiometers, J. Geophys. Res., 106, 12509–12526, 2001. 2792

Bais, A. F., Kazadzis, S., Garane, K., Kouremeti, N., Gröbner, J., Blumthaler, M., Seckmeyer, G., Webb, A. R., Koskela, T., Görts, P., and Schreder, J.: Portable device for characterizing the angular response of UV spectroradiometers, Appl. Optics, 44, 7136–7143, 2005. 2798

Bernhard, G. and Seckmeyer, G.: Uncertainty of measurements of spectral solar UV irradiance, J. Geophys. Res., 104, 14321–14346, 1999. 2792, 2794

Bernhard, G., Seckmeyer, G., McKenzie, R. L., and Johnston, P. V.: Ratio spectra as a quality control tool for solar spectral UV measurements, J. Geophys. Res., 103, 28855–28862, 1998. 2792

Bodhaine, B. A., Dutton, E. G., McKenzie, R. L., and Johnston, P. V.: Calibrating Broadband UV Instruments: Ozone and Solar Zenith Angle Dependence, J. Atmos. Ocean. Tech., 15, 916–926, 1998. 2796, 2813

Casale, G. R., Meloni, D., Miano, S., Palmieri, S., Siani, A. M., and Cappellani, F.: Solar UV-B irradiance and total ozone in Italy: Fluctuations and trends, J. Geophys. Res., 105, 4895–4902, 2000. 2792

Cheymol, A. and De Backer, H.: Retrieval of the aerosol optical depth in the UV-B at Uccle from Brewer ozone measurements over a long time period 1984-2002, J. Geophys. Res.,

AMTD

4, 2789–2826, 2011

First intercomparison of UV radiometers in Italy

H. Diémoz et al.

108, 4800–4809, 2003. 2795
CIE: Erythema reference action spectrum and standard erythema dose, Tech. rep., Commission Internationale de l'Éclairage, 1998. 2796, 2800
CIE: 134/1 TC 6-26 report: Standardization of the Terms UV-A1, UV-A2 and UV-B, Tech. rep., Commission Internationale de l'Éclairage, 1999. 2796, 2800
Di Menno, I., L. Moriconi, M., Di Menno, M., R. Casale, G., and Siani, A. M.: Spectral Ultraviolet Measurements by a Multichannel Monitor and a Brewer Spectroradiometer: A Field Study, Radiat. Prot. Dosim., 102, 259–263, 2002. 2792
di Sarra, A., Disterhoft, P., and DeLuisi, J.: On the Importance of Spectral Responsivity of Robertson-Berger type Ultraviolet Radiometers for Long-term Observations, Photochem. Photobiol., 76, 64–72, 2002. 2792
Diémoz, H. and Mayer, B.: UV radiation in a mountaineous terrain: comparison of accurate 3D and fast 1D calculations in terms of UV index, in: Proceedings UV conference, Davos, Switzerland, 18–20 September 2007, 165–166, 2007. 2798
Early, E. A., Thompson, E. A., and Disterhoft, P.: Field Calibration Unit for Ultraviolet Spectroradiometers, Appl. Optics, 37, 6664–6670, 1998. 2797
Glandorf, M., Arola, A., Bais, A., and Seckmeyer, G.: Possibilities to detect trends in spectral UV irradiance, Theor. Appl. Climatol., 81, 33–44, 2005. 2791
Gröbner, J. and Blumthaler, M.: Experimental determination of the reference plane of shaped diffusers by solar ultraviolet measurements, Opt. Lett., 32, 80–82, 2007. 2793
Gröbner, J. and Sperfeld, P.: Direct traceability of the portable QASUME irradiance scale to the primary irradiance standard of the PTB, Metrologia, 42, 134–139, 2005. 2794
Gröbner, J., Rembges, D., Bais, A. F., Blumthaler, M., Cabot, T., Josefsson, W., Koskela, T., Thorseth, T. M., Webb, A. R., and Wester, U.: Quality assurance of reference standards from nine European solar-ultraviolet monitoring laboratories, Appl. Optics, 41, 4278–4282, 2002. 2792
Gröbner, J., Schreder, J., Kazadzis, S., Bais, A. F., Blumthaler, M., Görts, P., Tax, R., Koskela, T., Seckmeyer, G., Webb, A., and Rembges, D.: Traveling reference spectroradiometer for routine quality assurance of spectral solar ultraviolet irradiance measurements, Appl. Optics, 44, 5321–5331, 2005. 2792, 2793, 2794
Gröbner, J., Blumthaler, M., Kazadzis, S., Bais, A., Webb, A., Schreder, J., Seckmeyer, G., and Rembges, D.: Quality assurance of spectral solar UV measurements: results from 25 UV monitoring sites in Europe, 2002 to 2004, Metrologia, 43, 66–71, 2006. 2792, 2804

Gröbner, J., Hülsen, G., Vuilleumier, L., Blumthaler, M., Vilaplana, J. M., Walker, D., and Gil, J. E.: Report of the PMOD/WRC-COST Calibration and Intercomparison of Erythemal radiometers, Tech. rep., COST Action 726, 2007. 2792, 2796, 2800

Gröbner, J., Hülsen, G., Wuttke, S., Schrems, O., De Simone, S., Gallo, V., Rafanelli, C., Petkov, B., Vitale, V., Edvardsen, K., and Stebel, K.: Quality assurance of solar UV irradiance in the Arctic., Photochem. Photobio. Sci., 9, 2010. 2792

Hülsen, G. and Gröbner, J.: Characterization and calibration of ultraviolet broadband radiometers measuring erythemally weighted irradiance, Appl. Optics, 46, 5877–5886, 2007. 2792, 2800

Ialongo, I., Casale, G. R., and Siani, A. M.: Comparison of total ozone and erythemal UV data from OMI with ground-based measurements at Rome station, Atmos. Chem. Phys., 8, 3283–3289, doi:10.5194/acp-8-3283-2008, 2008. 2792

JCGM: Evaluation of measurement data – Guide to the expression of uncertainty in measurement, Working Group 1 of the Joint Committee for Guides in Metrology, 2008. 2794

Kerr, J. B.: The Brewer Spectrophotometer, in: UV Radiation in Global Climate Change Measurements, Modeling and Effects on Ecosystems, 160–186, Tsinghua University Press, 2010. 2794

Kerr, J. B., McElroy, C. T., and Olafson, R. A.: Measurements of ozone with the Brewer spectrophotometer, in: Proceedings of the Quadrennial International Ozone Symposium, 74–79, 1980. 2794

Lantz, K., Disterhoft, P., Early, E., Thompson, A., DeLuisi, J., Kiedron, P., Harrison, Berndt, J., Mou, W., Erhamjian, T. J., Cabausua, L., Robertson, J., Hayes, D., Slusser, J., Bigelow, D., Janson, G., Beaubian, A., and Beaubian, M.: The 1997 North American Interagency Intercomparison of Ultraviolet Monitoring Spectroradiometers Including Narrowband Filter Radiometers, J. Res. Natl. Inst. Stan., 107, 19–62, 2002. 2792

Lantz, K., Disterhoft, P., Slusser, J. R., Gao, W., Berndt, J., Bernhard, G., Bloms, S., Booth, R., Ehramjian, J., Harrison, L., Janson, G., Johnston, P., Kiedron, P., McKenzie, R., Kimlin, M. G., Neale, P., O'Neill, M., Quang, V. V., Seckmeyer, G., Taylor, T., Wuttke, S., and Michalsky, J.: 2003 North American interagency intercomparison of ultraviolet spectroradiometers : scanning and spectrograph instruments, J. Appl. Remote Sens., 2, 1–33, 2008. 2792

Leszczynski, K., Jokela, K., Ylianttila, L., Visuri1, R., and Blumthaler, M.: Erythemally Weighted Radiometers in Solar UV Monitoring: Results from the WMO/STUK Intercomparison, Photochem. Photobiol., 67, 212–221, 1998. 2792

AMTD
4, 2789–2826, 2011

First intercomparison of UV radiometers in Italy

H. Diémoz et al.

Lucas, R., McMichael, T., Smith, W., and Armstrong, B.: Solar ultraviolet radiation - global burden of disease from solar ultraviolet radiation, Environmental Burden of Disease Series (WHO), 17, 2010. 2791

Madronich, S.: UV radiation in the natural and perturbed atmosphere, in: Environmental Effects of Ultraviolet Radiation, 17–69, Lewis, Boca Raton, Fla., 1993. 2798

Mayer, B. and Kylling, A.: Technical note: The libRadtran software package for radiative transfer calculations – description and examples of use, Atmos. Chem. Phys., 5, 1855–1877, doi:10.5194/acp-5-1855-2005, 2005. 2798

McKenzie, R. L., Bjorn, L. O., Bais, A., and Ilyasd, M.: Changes in biologically active ultraviolet radiation reaching the Earth's surface, Photoch. Photobio. Sci., 2, 5–15, 2003. 2791

Meloni, D., Casale, G. R., Siani, A. M., Palmieri, S., and Cappellani, F.: Solar UV Dose Patterns in Italy, Photochem. and Photobiol., 71, 681–690, 2000. 2792

Petkov, B., Vitale, V., Tomasi, C., Bonafé, U., Scaglione, S., Flori, D., Santaguida, R., Gausa, M., Hansen, G., and Colombo, T.: Narrow-band filter radiometer for ground-based measurements of global UV solar irradiance and total ozone, Appl. Optics, 45, 4383–4395, 2006. 2797

Schreder, J., Blumthaler, M., and Huber, M.: Design of an input optic for solar UV measurement, Internet Photochem. Photobiol., 1998. 2793

Seckmeyer, G., Bais, A., Bernhard, G., Blumthaler, M., Booth, C. R., Disterhoft, P., Eriksen, P., McKenzie, R. L., Miyauchi, M., and Roy, C.: Instruments to Measure Solar Ultraviolet Radiation, Part 1: Spectral Instruments, Tech. rep., World Meteorological Organization – Global Atmospherere Watch, 2001. 2791

Seckmeyer, G., Bais, A., Bernhard, G., Blumthaler, M., Booth, C. R., Lantz, K., and McKenzie, R. L.: Instruments to Measure Solar Ultraviolet Radiation, Part 2: Broadband Instruments Measuring Erythemally Weighted Solar Irradiance, Tech. rep., World Meteorological Organization – Global Atmospherere Watch, 1–41, 2008a. 2792

Seckmeyer, G., Pissulla, D., Glandorf, M., Henriques, D.and Johnsen, B., Webb, A., Siani, A. M., Bais, A., Kjeldstad, B., Brogniez, C., Lenoble, J., Gardiner, B., Kirsch, P., Koskela, T., Kaurola, J., Uhlmann, B., Slaper, H., Den Outer, P., Janouch, M., Werle, P., Gröbner, J., Mayer, B., De La Casiniere, A., Simic, S., and Carvalho, F.: Variability of UV Irradiance in Europe, Photochem. Photobiol., 84, 172–179, 2008b. 2792

Seckmeyer, G., Smolskaia, I., Pissulla, D., Bais, A. F., Tourpali, K., Meleti, C., and Zerefos, C.: Solar UV: Measurements and Trends, in: Twenty Years of Ozone Decline, edited by Zerefos,

AMTD

4, 2789–2826, 2011

First intercomparison of UV radiometers in Italy

H. Diémoz et al.

C., Contopoulos, G., and Skalkeas, G., 359–368, Springer Netherlands, 2009. 2791
Siani, A. M., Casale, G. R., Diémoz, H., Agnesod, G., Kimlin, M. G., Lang, C. A., and Colosimo, A.: Personal UV exposure in high albedo alpine sites, Atmos. Chem. Phys., 8, 3749–3760, doi:10.5194/acp-8-3749-2008, 2008. 2792
Siani, A. M., Casale, G. R., Sisto, R., Borra, M., Kimlin, M. G., Lang, C. A., and Colosimo, A.: Short-term UV Exposure of Sunbathers at a Mediterranean Sea Site, Photochem. Photobiol., 85, 171–177, 2009. 2792
Stamnes, K., Slusser, J., and Bowen, M.: Derivation of total ozone abundance and cloud effects from spectral irradiance measurements, Appl. Optics, 30, 4418–4426, 1991. 2797
UNEP: Environmental effects of ozone depletion and its interactions with climate change: 2010 assessment, Tech. rep., United Nations Environment Programme, 2010. 2791
Vanicek, K., Frei, T., Litynska, Z., and Schmalwieser, A.: UV-Index for the Public, a guide for publication and interpretation of solar UV Index forecasts for the public prepared by the Working Group 4 of the COST-713 Action UVB Forecasting, 1999. 2799
Webb, A., Gardiner, B. G., Martin, T. J., Leszczynski, K., Metzdorf, J., and Mohnen, V. A.: Guidelines for Site Quality Control of UV Monitoring, Tech. rep., World Meteorological Organization – Global Atmospherere Watch, 1998. 2792
Webb, A., Gardiner, B. G., Leszczynski, K., Mohnen, V., Johnston, P., Harrison, N., and Bigelow, D.: Quality Assurance in Monitoring Solar Ultraviolet Radiation: the State of the Art, Tech. rep., World Meteorological Organization – Global Atmosphere Watch, 2003. 2792
Webb, A., Gröbner, J., and Blumthaler, M.: A practical guide to operating broadband instruments measuring erythemally weighted irradiance, www.cost726.org, 2006. 2792, 2796
Webb, A. R., Slaper, H., Koepke, P., and Schmalwieser, A. W.: Know Your Standard: Clarifying the CIE Erythema Action Spectrum, Photochem. Photobiol., 87, 483–486, 2011. 2796
Williams, J. E., den Outer, P. N., and Slaper, H.: Quality assurance of solar spectral UV-measurements: methods and use of the SHICrivm software tool, in: EGS – AGU – EUG Joint Assembly, 2003. 2794
WMO: Scientific assessment of ozone depletion: 2010, Tech. rep., World Meteorological Organization, Global Ozone Research and Monitoring Project, 2011. 2791

AMTD
4, 2789–2826, 2011

First intercomparison of UV radiometers in Italy

H. Diémoz et al.

Table 1. Instruments and agencies participating to the comparison campaign. Regional (ARPA) and provincial (APPA) environmental protection agencies and research institutes as the university of Rome, the Italian National Research Council (CNR) and the Italian national agency for new technologies, energy and sustainable economic development (ENEA) were involved.

Id	Agency	Instrument	Ser. Num.	Type of meas.	Reference scale	Calib. date	Corrections	Temp. stab.
00	ARPA VdA	Bentham DTMc300F	5541	Spectral irr.	PMOD	2010	SHICrivm	Y
01	ARPA VdA	Kipp&Zonen UV-S-AE-T	000526	Broadband irr. (UV-A, UV-E)	Bentham ARPA VdA	2010	Spectral, angular (matrix)	Y
02	ARPA VdA	Kipp&Zonen UV-S-AE-T	040618	Broadband irr. (UV-A, UV-E)	Bentham ARPA VdA	2010	Spectral, angular (matrix)	Y
03	ARPA VdA	Yankee Env. Syst. UVB-1	020528	Broadband irr. (UV-E)	Bentham ARPA VdA	2010	Spectral, angular (matrix)	Y
04	ARPA Piemonte	Kipp&Zonen UV-S-AE-T	080003	Broadband irr. (UV-A, UV-E)	Kipp&Zonen	2009	Spectral, angular (matrix)	Y
05	ARPA Puglia	Kipp&Zonen UV-S-AE-T	080005	Broadband irr. (UV-A, UV-E)	Kipp&Zonen	2009	Spectral, angular (matrix)	Y
06	Sapienza Univ. Roma	Yankee Env. Syst. UVB-1	970827	Broadband irr. (UV-E)	PMOD	2006	Spectral, angular (matrix)	Y
07	IBIMET-CNR/ LaMMa	Solar Light 501A	5790	Broadband irr. (UV-E)	QASUME	2008	None (abs. factor)	Y
08	ENEA and ARPA Lazio	Solar Light 501A	13126	Broadband irr. (UV-E)	Brewer #123	2010	Spectral, angular (Bodhaine et al., 1998)	Y
09	APPA Bolzano	Solar Light digital 501	3733	Broadband irr. (UV-A)	Solar Light	2010	None (abs. factor)	Y
10	APPA Bolzano	Solar Light digital 501	2717	Broadband irr. (UV-E)	Solar Light	2010	None (abs. factor)	Y
11	ARPA VdA and Sapienza	Kipp&Zonen Brewer MKIV	66	Total ozone and spectral irr.	Bentham ARPA VdA	2010	Angular, straylight, temperature, SHI-Crivm	N
12	ISAC-CNR	ISAC UV-RAD filter rad.	N.A.	Narrowband irr. (7 channels)	Bentham ARPA VdA	2006	None	Y
13	ENEA and ARPA Lazio	ENEA F-RAD 02 filter rad.	N.A.	Narrowband irr. (13 channels)	Brewer #123	2010	None	Y
14	ARPA VdA	libRadtran 1.5 (model)	N.A.	Spectral irr.	N.A.	N.A.	N.A.	N.A.

AMTD
4, 2789–2826, 2011

Title Page
Abstract Introduction
Conclusions References
Tables Figures
◀ ▶
Back Close
Full Screen / Esc
Printer-friendly Version
Interactive Discussion

Table 2. Radiometric uncertainty (%) of the spectroradiometer. The total radiometer uncertainty is calculated as the squared sum of the different contributions.

Contribution	300 nm	310–400 nm
Lamp certificate (PMOD)	2.3	2.3
Instability	0.4	0.4
Statistic noise	0.2	0.1
Non-linearity	0.5	0.5
Current	0.1	0.1
Lamp aging	0.5	0.5
Wavelength misalignment	0.1	0.1
Heating of the diffuser	1.0	1.0
Total	2.7	2.7

AMTD
4, 2789–2826, 2011

Table 3. Total uncertainty (%) of the spectroradiometer. The total radiometer uncertainty is calculated as the squared sum of the different contributions.

Contribution	300 nm 50°	300 nm 75°	310–400 nm 50°	310–400 nm 75°
Radiometric uncertainty	2.7	2.7	2.7	2.7
Diffuser temperature	0.6	0.6	0.6	0.6
Angular response	0.4	0.4	0.8	0.8
Non-linearity	0.5	0.5	0.5	0.5
Instability	0.4	0.4	0.4	0.4
Statistic noise	0.8	4.6	0.3	0.9
Wavelength misalignment	2.1	2.4	2.1	0.9
Total	3.6	5.9	3.0	3.2
Expanded (K=2)	7.2	12	6.0	6.4

AMTD
4, 2789–2826, 2011

Table 4. Input parameters to the radiative transfer model.

Parameter	Value
Solar spectrum	Atlas-3 plus Modtran
Atmosphere	Standard midlatitude summer
Aerosol	Default (Shettle 1989, rural type)
SSA	Default reduced by 10 %
Angstrom parameters	α 1.5, β from Brewer
Ozone cross sections	Molina & Molina 1986
Number of streams	12
Altitude	570 m a.s.l.
Total ozone	Brewer measurements
Effective albedo	3 %
Pressure	950 hPa
Solver	Pseudospherical disort (sdisort)

AMTD
4, 2789–2826, 2011

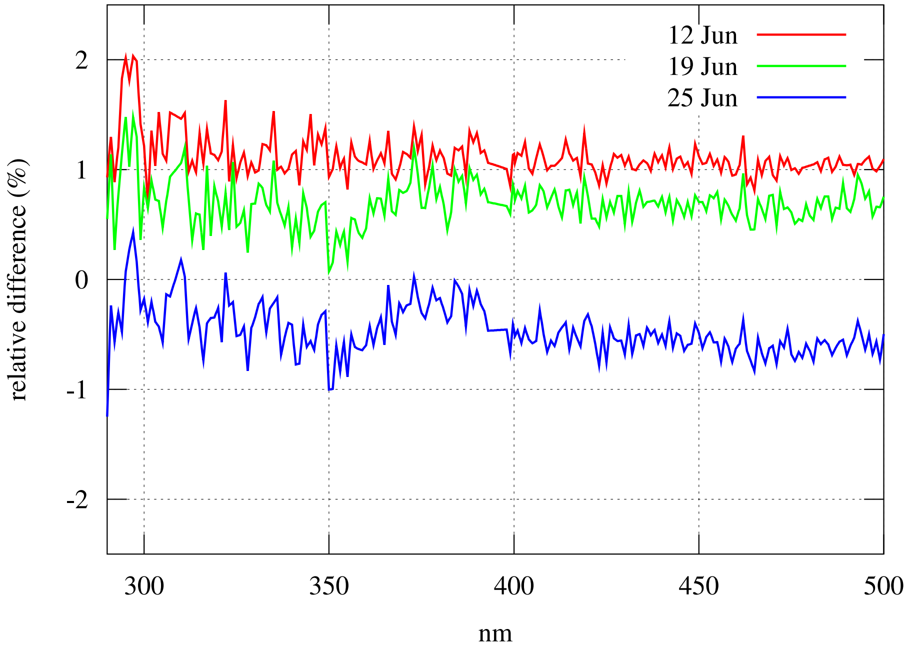

Fig. 1. Percentage variations of the spectroradiometer spectral responsivity relative to the first calibration in the campaign (4 June 2010). Every calibration curve is obtained as an average of the responsivities measured with three lamps.

AMTD
4, 2789–2826, 2011

First intercomparison of UV radiometers in Italy

H. Diémoz et al.

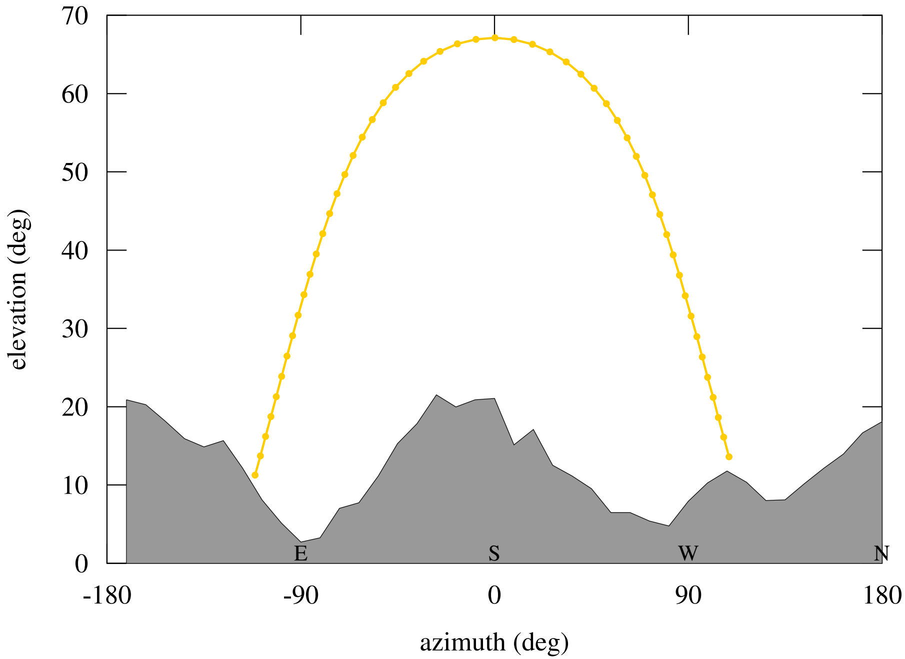

Fig. 2. Horizon and sun elevation at Saint-Christophe. The sun trajectory for 8 June is drawn from 5 UT to 17.45 UT. Circles are plotted every 15 min.

AMTD
4, 2789–2826, 2011

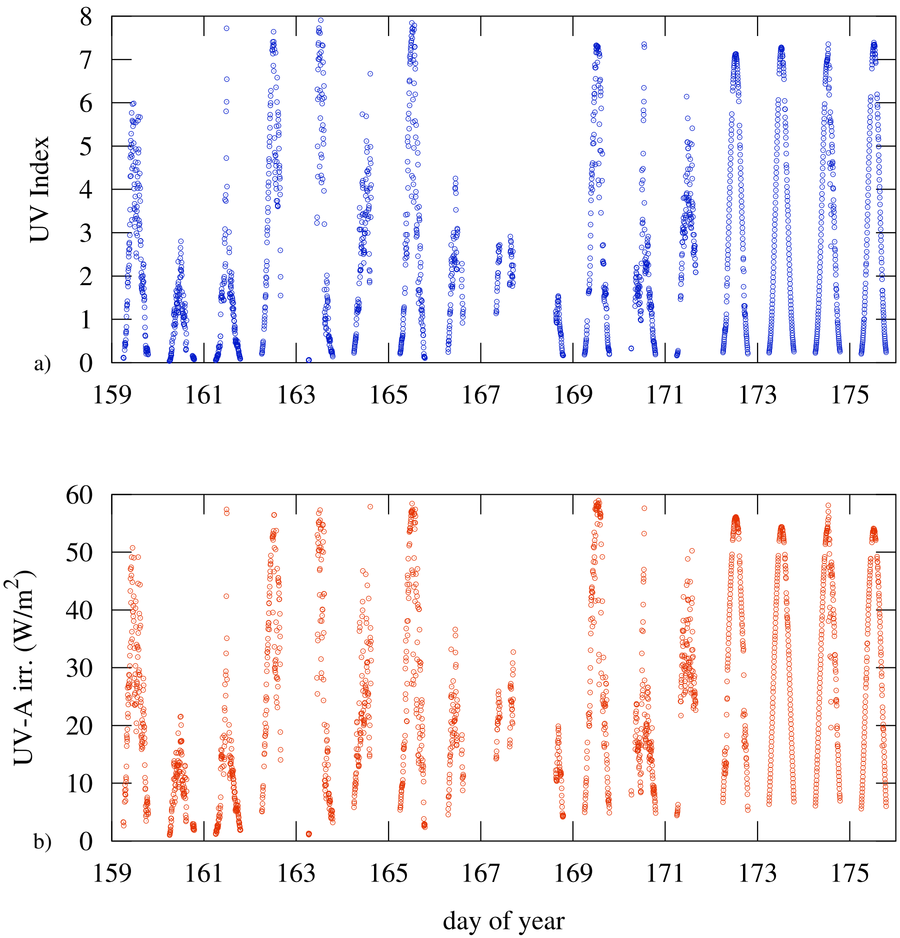

Fig. 3. Time series of Bentham measurements: **(a)** global solar UV Index and **(b)** broadband UV-A irradiance. Missing data occurs in rainy periods, before sunrise, after sunset, during calibrations and dome cleaning.

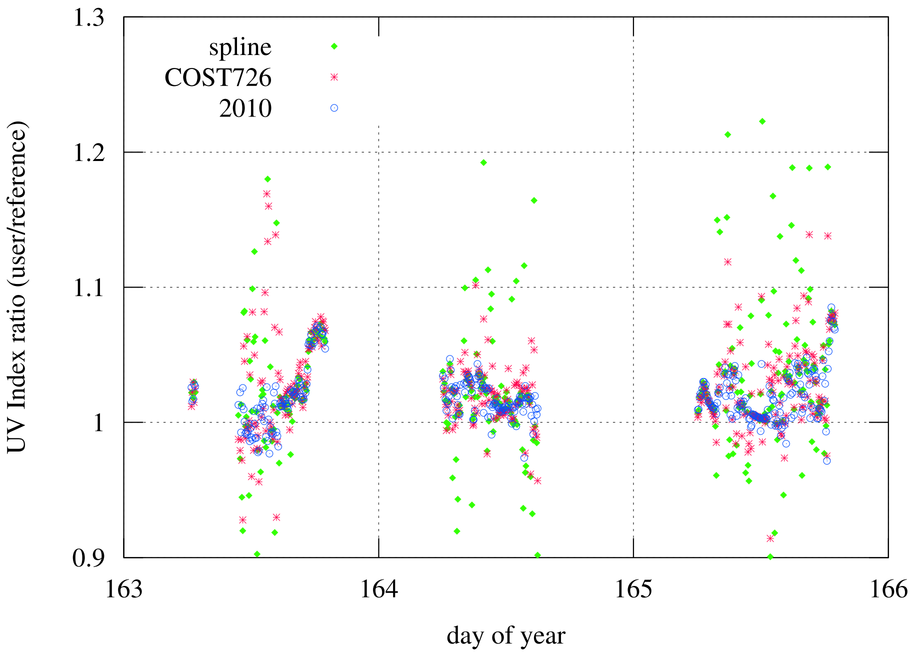

Fig. 4. Comparison of several methods to downscale the broadband data. The graph shows the ratio of the broadband irradiance measured with instrument 01 and the reference during three cloudy days. Cubic spline interpolation is represented with green diamonds, the COST Action 726 algorithm with red asterisks and the algorithm used in this study with blue circles.

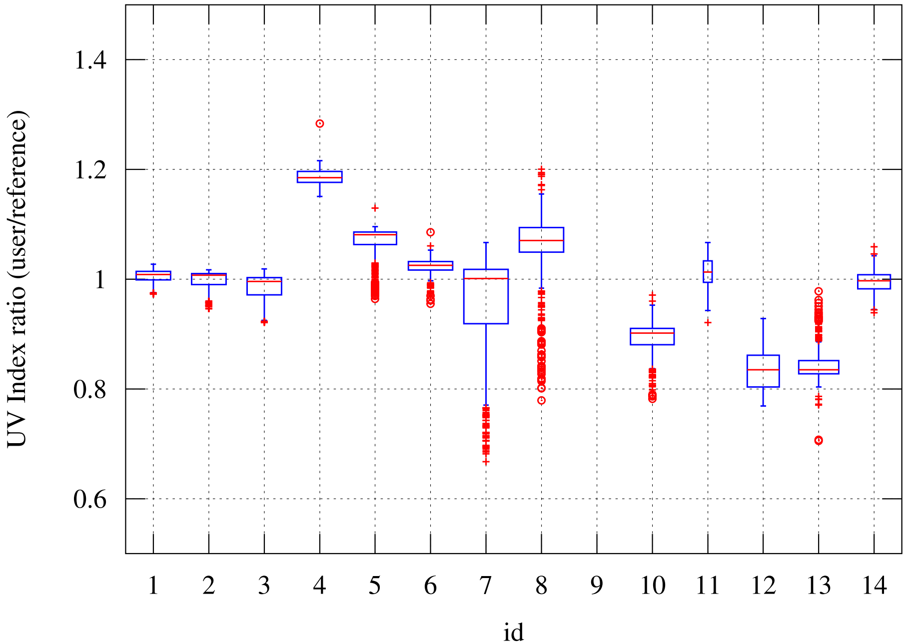

Fig. 5. Boxplot of UV Index ratios between each instrument and the reference, calculated under clear sky conditions. The top and the bottom of the boxes represent respectively the upper and the lower quartiles. The lines inside the boxes depict the median. The whiskers show minimum and maximum values except the outliers, which are drawn as cross (between 1.5 and 3 times the IQR) and circles (beyond 3 times the IQR). Instrument id 09 does not measure the UV Index.

AMTD

4, 2789–2826, 2011

First intercomparison of UV radiometers in Italy

H. Diémoz et al.

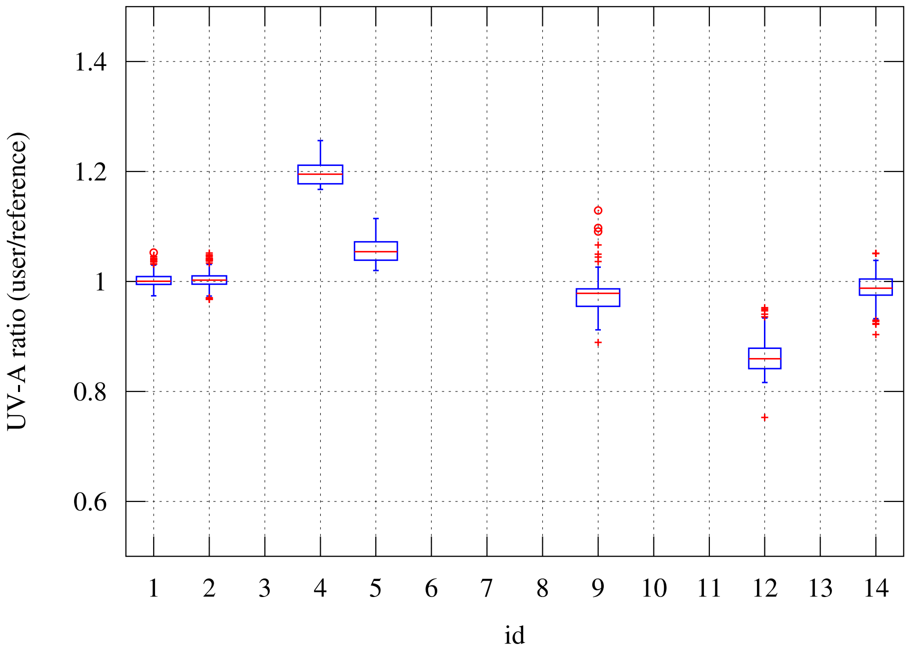

Fig. 6. Boxplot of broadband UV-A irradiance ratios between each instrument and the reference, calculated under clear sky conditions. Only instruments measuring UV-A irradiance can be shown in the graph.

AMTD
4, 2789–2826, 2011

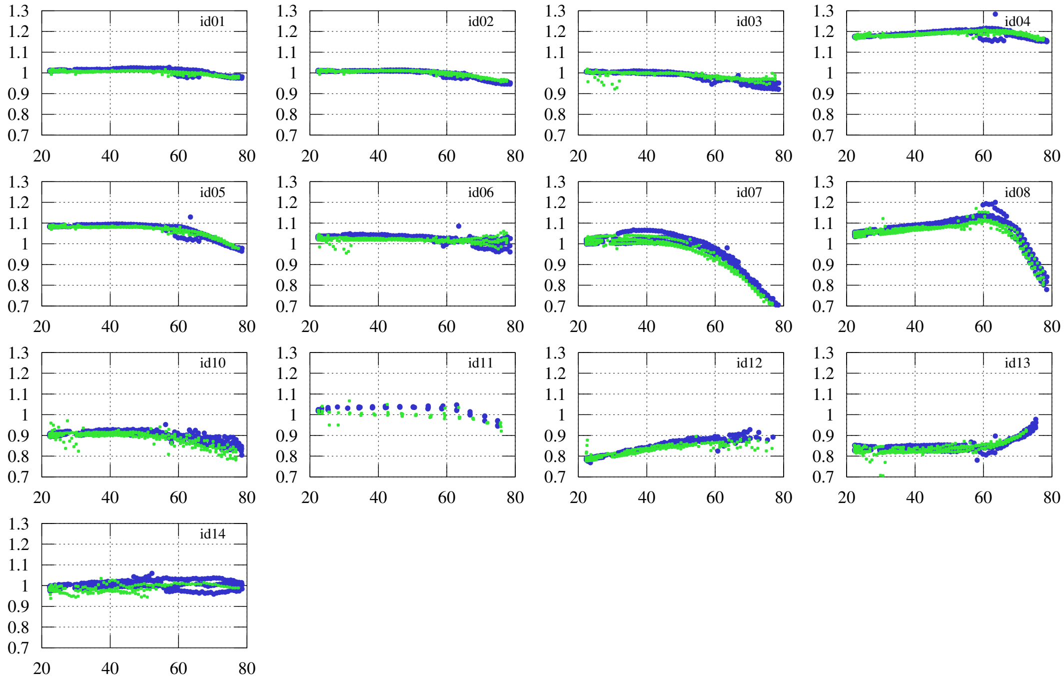

Fig. 7. Ratios between UV Index measurements with user instruments and the reference (vertical axis) against the solar zenith angle (horizontal axis). Morning (blue) and afternoon (green) measurements are plotted separately.

AMTD
4, 2789–2826, 2011

First intercomparison of UV radiometers in Italy

H. Diémoz et al.

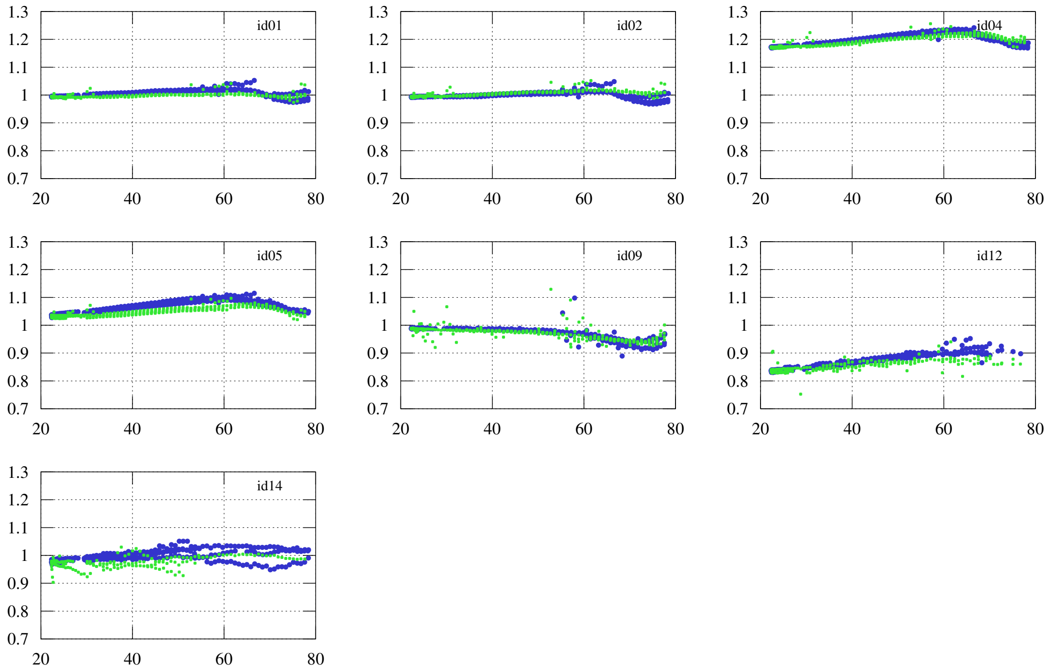

Fig. 8. Ratios between broadband UV-A irradiance measurements with user instruments and the reference (vertical axis) against the solar zenith angle (horizontal axis). Morning (blue) and afternoon (green) measurements are plotted separately.

AMTD
4, 2789–2826, 2011

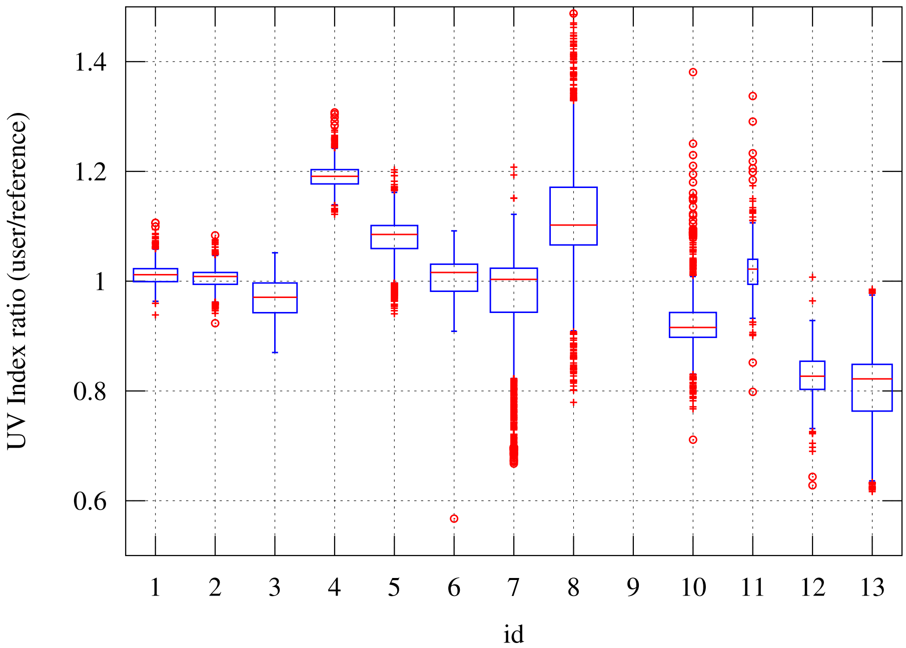

Fig. 9. Boxplot of UV Index ratios between each instrument and the reference, calculated under all sky conditions (both cloudy and clear days). The clear-sky simulations (id 04) were not considered in the analysis.

AMTD
4, 2789–2826, 2011

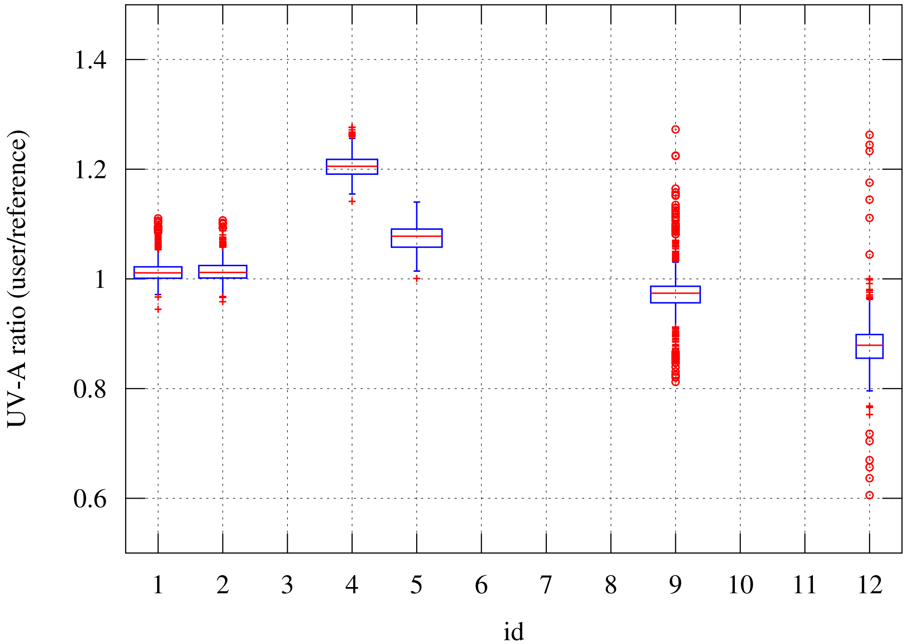

Fig. 10. Boxplot of broadband UV-A irradiance ratios between each instrument and the reference, calculated under all sky conditions (both cloudy and clear days).